Rheol Acta (2016) 55:527–536
DOI 10.1007/s00397-016-0936-5

ORIGINAL CONTRIBUTION

Measuring average rheological quantities of cell monolayers in the linear viscoelastic regime

Haider Dakhil[1,2] · Daniel F. Gilbert[3,4] · Deepika Malhotra[1,5] · Anja Limmer[1,6] · Hannes Engelhardt[6] · Anette Amtmann[6] · Jan Hansmann[5] · Holger Hübner[6] · Rainer Buchholz[4,6] · Oliver Friedrich[3,4] · Andreas Wierschem[1,4]

Received: 2 March 2015 / Accepted: 21 April 2016 / Published online: 28 April 2016

Abstract During the last decades, the rheology of cells has been studied almost entirely in single cells. While cell-to-cell variation is typically very large and most studies were carried out in the nonlinear viscoelastic regime, we quantify average linear viscoelastic cell properties like storage and loss moduli and normal stress in monolayers of different cell types showing that murine 3T6 fibroblasts, human fibroblasts, and HeLa cells differ considerably in their storage modulus. To this end, we modified a commercial rheometer to set up a parallel-disk configuration at gap widths of a few micrometers and optically detected the cell concentration in the gap. This enables studying the linear viscoelastic behavior of the cells and permits quantifying the impact of drugs affecting the cytoskeleton or the extracellular matrix connection. Thus, due to its high-content approach, without the need of treating the samples in the rheometer, this envisions the use of this method as a fast diagnostic tool. The method also allows for quantitatively studying of the impact of pre-stress on the storage and loss moduli of the cells.

Keywords Cell rheology · Linear viscoelasticity · Narrow-gap rheometry · Parallel-disk configuration · Cell monolayer · Biochemical treatment · Pre-stress · Primary cells · Cell lines

✉ Andreas Wierschem
andreas.wierschem@fau.de

[1] Institute of Fluid Mechanics, Friedrich-Alexander-Universität Erlangen-Nürnberg FAU), Cauerstr. 4, 91058 Erlangen, Germany

[2] Faculty of Engineering, University of Kufa, Kufa, P.O. Box 21, Najaf 00964, Iraq

[3] Institute of Medical Biotechnology, Friedrich-Alexander-Universität Erlangen-Nürnberg (FAU), Paul-Gordan-Str. 3, 91052 Erlangen, Germany

[4] Erlangen Graduate School in Advanced Optical Technologies (SAOT), Friedrich-Alexander-Universität Erlangen-Nürnberg (FAU), 91052 Erlangen, Germany

[5] Fraunhofer Institute for Interfacial Engineering and Biotechnology, IGB Röntgenring 11, 97070 Würzburg, Germany

[6] Institute of Bioprocess Engineering, Friedrich-Alexander-Universität Erlangen-Nürnberg (FAU), Paul-Gordan-Str. 3, 91052 Erlangen, Germany

Introduction

Rheological properties of biological cells have vital functional implications such as mechanical stability, adjustment to environmental load, migration, proliferation, phagocytosis, and contraction and are important, for instance, for health-care products and vaccines (Kollmannsberger and Fabry 2009). The mechanical properties of the cell are closely related to their physiological activities. Cancer, for example, changes the mechanical cell properties, and blood cells are only able to transport oxygen through narrow blood capillaries by changing their shape (Niu and Cao 2014). In eukaryotic cells, the cytoskeleton, which is a contractile network of protein filaments covering the entire cell body, is responsible for controlling the mechanical properties, cell shape, locomotion, and division (Kollmannsberger and Fabry 2011). The cytoskeleton itself is a complex protein-gel that has the ability to support large elastic stresses. At the same time, it is able to generate internal stresses.

Due to its importance for our general understanding of cells and countless applications in biotechnology, bioengineering, and medicine, great effort has been put into studying the rheological behavior of cells. During the last decades, different techniques, like optical and magnetic tweezers, atomic force microscopy, magnetic twisting cytometry,

micropipettes, microplates, cell poking, and particle tracking microrheology, have been employed to measure the viscoelastic behavior of single cells. For an overview, see, for instance, Verdier et al. (2009) and Kollmannsberger and Fabry (2011).

Studies on the viscoelastic properties of single cells have been carried out at frequencies up to about 10^4 Hz. Over a wide frequency range, cells exhibit a power-law rheology like soft glassy materials. The exponents typically range between 0.1 and 0.5. They are smaller for stiffer cells (for an overview, refer to Kollmannsberger and Fabry 2011). At frequencies below 0.1 Hz, a second branch with higher exponent may occur (Stamenović et al. 2007; Verdier et al. 2009).

Depending, for instance, on cell identity, life cycle, shape, structure, and level of proteins (Weissman-Shomer and Fry 1975), cells show large cell-to-cell variations. The stiffness and dynamic moduli may vary by orders of magnitude (Cai et al. 2013). On the other hand, drugs, aging, or diseases may strongly affect the cytoskeleton and thus the viscoelastic cellular properties (Lekka et al. 1999; Guck et al. 2005; Schulze et al. 2010). Hence, to quantify their impact, it is of great importance to determine average values for the viscoelastic cell properties in the linear viscoelastic range. While in single-cell studies, experiments with several tens up to about 200 cells have been carried out (Mierke et al. 2008; Cai et al. 2013), averaging over a large number of cells may be achieved by studying them in a monolayer between rheometer disks (Fernández et al. 2007; Elkins et al. 2015). In the present work, using a narrow-gap rotational rheometer (Dakhil and Wierschem 2014) and detecting the cell coverage in the monolayer, we show that the linear viscoelastic regime can be reached and average cell moduli can be determined from a substantial number of cells at once. The setup can be used to quantify the impact of biochemical treatments on the cells in a single experimental run that would otherwise be difficult to determine in low-content methodologies (e.g., micropipette aspiration) on the background of strong cell-to-cell variations. Hence, this method may also be used as a diagnostic tool to identify variations in the rheological cell behavior, for instance, in transgenic cell lines. Furthermore, changing the gap width allows studying the rheological behavior of the cells under pre-set stress conditions.

For monolayers of cells with typical length scales in the order of 10 μm, the absolute gap width between the rheometer plates and their parallelism have to be controlled with a precision of about 1 μm. This is beyond the scope of commercial rheometers that usually have a systematic error in the gap width of about 25 μm and more (Davies and Stokes 2005; Davies and Stokes 2008; Pipe et al. 2008). To meet these requirements, we recently modified a commercial rotational rheometer to ensure not only parallelism of both plates at a given position but also to align both plates perpendicularly to the rotating axis with unprecedented precision. This enables, for instance, larger deformations, shear rates of 10^5 s^{-1} and studies with low viscous media at gap widths of about 10 μm (Dakhil and Wierschem 2014).

In the present article, we quantify the rheological properties of fibroblasts of different origin and HeLa cells. First, we explore the abilities of the method with murine fibroblasts, before we compare their rheological properties to human primary fibroblasts and HeLa cells. Fibroblasts are part of the connective tissue and maintain its structural integrity by continuously secreting precursors of the extracellular matrix, i.e., collagen (Weissman-Shomer and Fry 1975). They play a vital role in adapting viscoelastic properties of tissue (Tuan et al. 1996) and are required in the wound healing process as a regenerative pool for extracellular matrix production (Grinell 1994). Murine and human skins are anatomically and biomechanically similar (Karimi et al. 2015). Yet, transferring from animal to human cells on a quantitative level might be questionable. Furthermore, despite many advantages of cell lines, such as high availability or consistent cell properties, cell lines differ from the in vivo situation (Unger et al. 2002; Pan et al. 2009). To see how much this may affect the linear viscoelastic properties, we compare the murine 3T6 fibroblast cell line to human primary cells. Cancer cells, on the other hand, are more deformable than normal cells (Guck et al. 2005). While Guck et al. (2005) studied rather large deformations, we focus here on the linear viscoelastic properties. As an example for cancer cells, we study HeLa cells. They were the first continuous cancer cell line established in 1951 from the epitheloid cervix carcinoma of a 30-year-old woman (Gey et al. 1952; Lucey et al. 2009). This cell line helped to study characteristics and treatment strategies of cancer in vitro. HeLa cells are still the most widely used human cancer cell line and are thus of paramount importance (Masters 2002). Due to its tissue origin, this cell line grows in vitro epithelial-like in monolayers. Current cancer treatment strategies focus inter alia on the cytostatic effect of microtubule-stabilizing agents.

Materials and methods

We used 3T6 Swiss albino murine fibroblasts and the human cervix carcinoma cell line HeLa (ACC 57) from the German Collection of Microorganisms and Cell Cultures (DSMZ), Braunschweig, Germany. Primary human dermal fibroblasts were isolated from foreskin biopsies from a 3-year-old donor under informed consent according to ethical approval granted by the institutional ethics committee of the Julius-Maximilians-University, Wuerzburg, Germany. The study was approved by the ethics committee (vote 182/10). Additionally, informed and written consent from the next of kin, caretakers, or guardians on behalf of the children was obtained. The biological properties of murine fibroblasts are described by Todaro and Green (1963). After thawing the cells

from cryostorage, the murine fibroblasts were grown in an incubator at a temperature of 310.16 K for at least 1 week and no longer than 1 month following the protocol from Freshney (1993). As culture medium, we used Dulbecco's modified Eagle medium (DMEM, Invitrogen) with 10 % (*v*/*v*) fetal bovine serum (FBS), 25 mM HEPES, and 0.5 mM $NaHCO_3$ (Sigma-Aldrich). Cells were cultured at a temperature of 298.16 K and were passaged weekly. The human fibroblasts were cultured in DMEM ((1×) + GlutaMAX-I, Life Technologies) supplemented with 10 % (*v*/*v*) fetal calf serum (FCS, Biochrom) and an antibiotic combination of 1 % Pen Strep (Sigma-Aldrich), at pH 7.4, 310.16 K, and 5 % CO_2. The cells were grown in 150 cm^2 tissue culture flasks with 500,000 cells. Medium was changed every 2–3 days. Cells were passaged when the confluency reached 90 %. For passaging, after removing the medium, the cells were detached with Accutase solution and centrifuged at 256*g* for 5 min before diluting the cells in fresh medium. The HeLa cells were cultured in 25 cm^2 tissue culture flaks in RPMI 1640 medium (Life Technologies) supplemented with 10 % (*v*/*v*) fetal bovine serum (FBS) and 4 mM L-glutamine at pH 7.4, 310.16 K, and 5 % CO_2. For passaging, the spent medium was removed and the cells were detached with 2 ml Accutase solution and centrifuged at 180*g* for 8 min. Cells were diluted in fresh medium to a final volume of 7.5 ml with a cell concentration of 30,000 cells/cm^2. Cultures were used up to 3 months.

The experiments were performed with a UDS 200 rotational rheometer from Physica at temperatures of (296.56 ± 0.1 K) (mouse fibroblasts), (297.11 ± 0.8 K) (human fibroblasts), and (296.86 ± 1.5 K) (HeLa). As bottom plate, we used a glass plate of 75 mm diameter with an evenness of 1λ (Melles Griot) or λ/4 (Edmund Optics), where λ is the testing wavelength (633 nm). As rotating plate, we used glass plates that were glued to a measurement head of the rheometer. In the studies with murine fibroblasts and HeLa cells, plate diameter and evenness was 50 mm and λ/20 (Melles Griot). The human fibroblasts were studied with a plate of 25 mm diameter and an evenness of λ/10 (Edmund Optics). To align the bottom plate perpendicularly to the rotation axis, it was fixed to a tripod, which was mounted to the rheometer table. The tripod was aligned with 3 micrometer screws and fixed to the rheometer with three screws after adjustment.

To work in the parallel-disk configuration at gap widths of about 5 μm, zero-point errors have to be reduced considerably, and the plates have to be aligned in parallel to each other and perpendicularly to the rotational axis. This was achieved with a confocal interferometric sensor resulting in a gap width with a precision of about ±0.7 μm. Hence, the error in zeroing the gap is avoided and the real gap width is validated correctly and independently from the rheometer reading. For further details about this approach, we refer to Dakhil and Wierschem (2014).

To quantify the cell coverage in the gap, the cells were visualized from underneath with a camera equipped with a 5× objective lens. Forty fluorescence images and, occasionally, transillumination images at a field-of-view of 0.775 mm^2 were taken around the edge of the upper plate. As light source, we used light-emitting diodes, VLP IntraLED 2020/W (Volpi) connected to a light guide (Lumatec 3716) for transillumination images and LUXEON Rebel (Lumitronix) for fluorescence images. The latter was mounted to a filter block (C-FL Epi-FL FITC, EX 465-495, DM 505, BA 515-555, Olympus), which was incorporated in the lens tube. The pictures were grabbed with a CCD camera with a primary resolution of 1280 × 960 pixels (1.3 MP Chameleon, 1/3″ CCD, Point Grey Research). Images of fluorescent cells were segmented and quantitatively analyzed using a modified version of DetecTIFF® software. For further details about the software, we refer to Gilbert et al. (2009). Since deformation is strongest at a maximum distance from the rheometer's turning axis, the rheometer signal is mainly due to the cells at the outer rim. Figure 1 shows a sketch of the setup.

The cells were prepared for the rheological experiments as follows: The culture medium was removed from the culture flask. The flask with the murine fibroblasts was rinsed with 5 ml of phosphate-buffered solution (PBS) buffer, gently shaken, and PBS was removed and discarded. Five milliliters of Accutase solution (Sigma-Aldrich) was added and the flask was incubated at room temperature for 30 min. For human fibroblasts, the quantities for PBS and Accutase were doubled. These cells were incubated in CO_2 for 10 min. In the case of HeLa cells, Accutase solution was added directly after removing the medium and the flask was put into the incubator for 10 min. It was checked under an inverted microscope if at least 90 % of the cells were detached and floating. Detached cells were identified by their round shape. Ten milliliters of culture medium was added to the culturing flask to inactivate the trypsin, and cells were removed and transferred into a 50-ml conical tube and spun-down for 8 min at 180*g* (murine fibroblasts and HeLa cells) or at 256*g* for 5 min (human fibroblasts). The supernatant was discarded and the cells in the pellet were counted after resuspension using a hemocytometer to estimate the amount of cells needed in each individual experiment.

To optically determine the cell coverage in the rheometer gap, we added 0.02 vol.% of the fluorescent agent Calcein AM (Sigma-Aldrich) to the cells. Calcein AM is a membrane-permeable fluorescein derivative able to diffuse into cells. Upon cell entry, Calcein AM is de-esterified and thereby modified into the green fluorescent Calcein. This fluorescent signal can be monitored using appropriate filter sets (485 nm excitation/530 nm emission wavelength). After modification, the molecule is no longer able to diffuse out of the cell. Cell staining was carried out for about 1 h at a temperature of 310.16 K. Upon fluorescence labeling, the cells were centrifuged at 180*g*, the staining solution was replaced by 2 ml culture medium to entirely remove Calcein AM from the

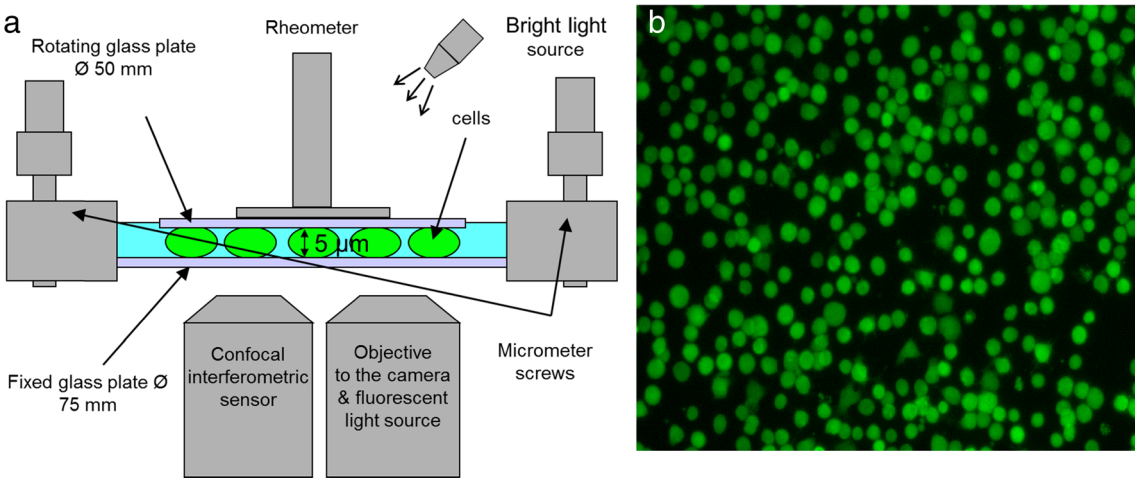

Fig. 1 Sketch of the setup in the customized rheometer (**a**) and fluorescence image of the cells (**b**). The gap width between the rheometer plates is measured with a confocal interferometric sensor; the cells are viewed with a camera. Cell coverage in (**b**), 42 %

extracellular medium. To detect dead cells, we added 0.01 vol.% of the fluorescent agent propidium iodide (Sigma-Aldrich) to the cells. Propidium iodide is a widely utilized fluorescence stain in cell culture (488 nm excitation/615 nm emission wavelength). It intercalates to all double-stranded nucleic acids. Viable cells with intact plasma membrane exclude propidium iodide. Therefore, it can be used as a viability marker to discriminate viable and nonviable cells (Sasaki et al. 1987). To determine the number of dead cells, we used the same fluorescence microscope as described above with a TRITC filter block (EX 526-552, EM 594-646).

The rheometer glass plates were coated with a fibronectin solution in order to promote cell adhesion to the plates. The solution usually consisted of 30 μg ml^{-1} fibronectin (Sigma-Aldrich), an adhesion-promoting protein, dissolved in PBS. To minimize cell detachment in studies with elongated cells, we increased the amount of fibronectin to 100 μg ml^{-1}. The solution was left between the glass plates for 1 h at a gap width of 50 μm. In case of the fibroblasts, the plates were rinsed with PBS. Therefore, the upper plate was lifted up and down and the solution was sucked into a pipette.

The suspension of fluorescence labeled cells was pipetted onto the lower glass plate of the rheometer and was left for 20 min to let the cells settle down and adhere to the plate. Thereafter, the upper glass plate of the rheometer was lowered at minimum speed of the rheometer to confine and compress the cells, ensuring that practically all cells adhered well to both plates. The cells were left in this position for another hour to promote adhesion between both plates. Thereafter, the gap width was adjusted to the desired gap width, which is chosen to be close to the average height of the cells. Unless otherwise specified, the gap width was fixed at 5 μm for mouse fibroblasts and at 14 μm for HeLa cells. Passages of the human fibroblasts varied in mean size. They were studied at gap widths where the normal force was about zero. Images were taken to determine the cell coverage in the gap before commencing rheological measurements. Excess cell suspension covered the entire bottom and the gap. It was not removed to avoid drying from the edges.

To clarify the impact of the nuclei on the rheological measurements, we recorded the rheological properties of cells in the presence of blebbistatin. Blebbistatin inhibits myosin motors that can generate contraction in the actin network (Kovács et al. 2004). We treated the cells with 150 μmol blebbistatin (Sigma-Aldrich). To allow good interaction of this drug with the cells, it was mixed into the culture medium just before leaving the cells between the glass plates.

Experimental results

Unless otherwise specified, the frequency was fixed at 1 Hz. Representative amplitude sweeps are shown in Fig. 2. The data is characteristic for viscoelastic solids. As shown in the diagrams, the linear viscoelastic regime ranges up to strain amplitudes of about 1 %. Note that the scatter at low strain amplitudes of about 0.1 % is due to the torque limit of the rheometer; see Oliveira et al. (2006) and Soulages et al. (2009) for a discussion on a realistic lower limit. The torque limit results in strong scatter at correspondingly larger amplitudes for lower moduli. Yet, the scatter for the loss modulus of the fibroblasts at larger strain amplitudes in Fig. 2a is apparently not due to the torque limit as shown in a comparison to the HeLa cells in Fig. 2b. Although the HeLa cells have much smaller moduli, the data scatter less. The same holds for fibroblasts at larger gap widths.

To quantify how long-term changes of the cell properties due to aging may affect the rheological measurements, we recorded the moduli of mouse fibroblasts for about 10 h. During the test, the cells were exposed to a constant deformation amplitude of 0.2 % at a frequency of 1 Hz. As shown in Fig. 3, the storage and loss moduli increased during the test by about a factor of 1.5 and 1.15, respectively. The subsequently

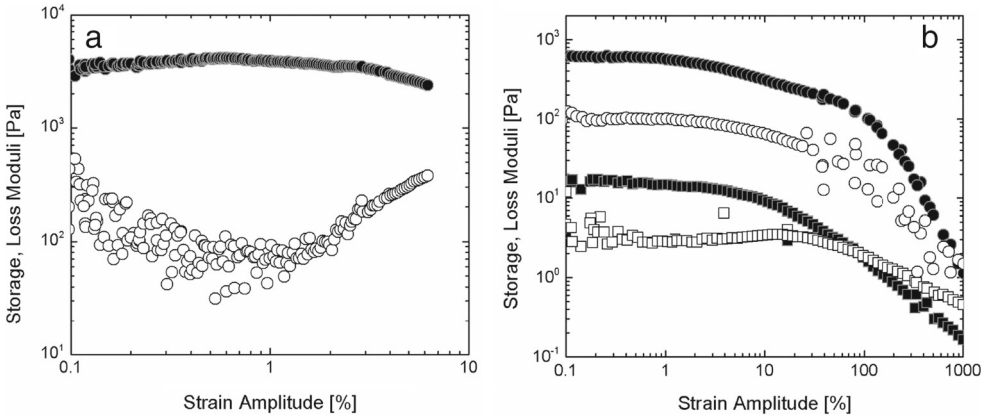

Fig. 2 Amplitude sweep of mouse fibroblasts at a gap width of 5 μm (**a**) and of HeLa cells at a gap width of 14 μm (**b**) at a frequency of 1 Hz. Storage modulus and loss modulus of the cells in cell culture medium are indicated by *closed* and *open circles*, respectively. In (**b**), the moduli of the cell culture medium are indicated by *squares*

reported amplitude and frequency sweeps usually took about 30 min. During this time, the moduli hardly change within measurement uncertainty. Only the study on the impact of the gap width (Figs. 5 and 6) took about 4.5 h. We also detected with propidium iodide the number of dead HeLa cells and how the experimental conditions affect it. While dead cells accounted for less than 1 % of the total just at the beginning of cell compression, the number of dead cells increased to about 1.5 % after 1 h of compression and barely altered during the sweeps.

Figure 4a shows the storage and loss moduli of the murine fibroblasts in the linear viscoelastic regime for different cell coverages up to about 50 % of the area in the gap. At higher cell concentrations, cell agglomeration becomes significant making it difficult to obtain a monolayer. The value of the loss modulus in the linear viscoelastic range was determined by averaging the loss modulus around the minimum at strain amplitudes between 0.3 and 1 %; see Fig. 2a. The error bars for the moduli indicate the standard deviation for the linear viscoelastic regime. The error bars for the cell coverage show the standard deviation between the 40 locations around the outer part of the gap. The moduli of the cell monolayer strongly depend on the cell coverage. Figure 4a shows that the storage modulus is proportional to the cell coverage within the rheometer gap. As shown in Fig. 2b, the storage modulus of the medium, G'_{medium}, and its loss modulus, G''_{medium}, are much smaller than those of the cell monolayers, G′ and G″. Knowing the moduli of the medium, the average moduli of the cells, $\langle G'_{\mathrm{cell}} \rangle$ and $\langle G''_{\mathrm{cell}} \rangle$, can be determined from the measured moduli and the mean cell coverage close to the gap rim, *c*.

$$\left\langle G'_{\mathrm{cell}} \right\rangle = \frac{G' - (1-c) G'_{\mathrm{medium}}}{c} \tag{1}$$

Figure 4b shows the average storage modulus of the cells obtained in this way. The average moduli per cell fall within a narrow interval. The dashed lines indicate the mean values of the data points for the respective moduli. In particular, the data for the storage modulus per cell scatters around a mean value of about 17,000 Pa with standard deviation of about 19 %. The scatter is relatively large at small cell coverage. A cell coverage of about 30–50 % seems to be optimal. For the data in this range, the standard deviation reduces to about 13 %.

The method enables studying how externally applied prestress affects the dynamic cell moduli. To see how sensitive the viscoelastic cell properties depend on the pre-stress, we changed the gap width after adhering the cells to both plates. The experiment started by zeroing the normal force before bringing the upper plate into contact with the cell suspension. This permits quantifying the pre-stress exerted on the cells in the monolayer at different gap widths. Thereafter, the murine fibroblasts were confined at a gap width of 5 μm. At this gap width, we carried out an amplitude sweep at a frequency of 1 Hz and at strain amplitudes between 0.1 and 5 % to determine the linear viscoelastic range. Thereafter, frequency sweeps between 0.1 and 10 Hz were carried out in the linear viscoelastic range at a strain amplitude of 0.2 % for the different gap widths that were increased stepwise up to 16 μm. At the end of the experiment, an amplitude sweep and a frequency sweep were carried out again at a width of 5 μm to quantify changes during the experimental run.

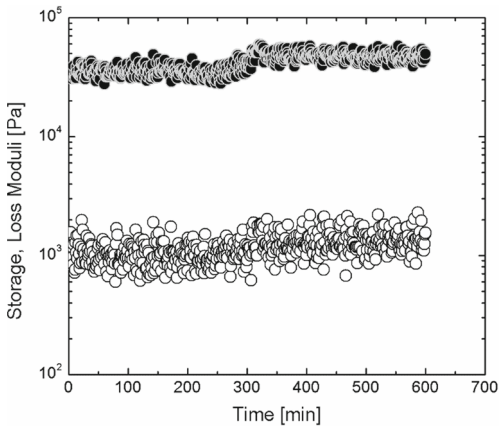

Fig. 3 Aging test for the murine fibroblast cells with constant strain amplitude of 0.2 % and constant frequency of 1 Hz at a gap width of 5 μm. Storage modulus and loss modulus are indicated by *closed* and *open symbols*, respectively

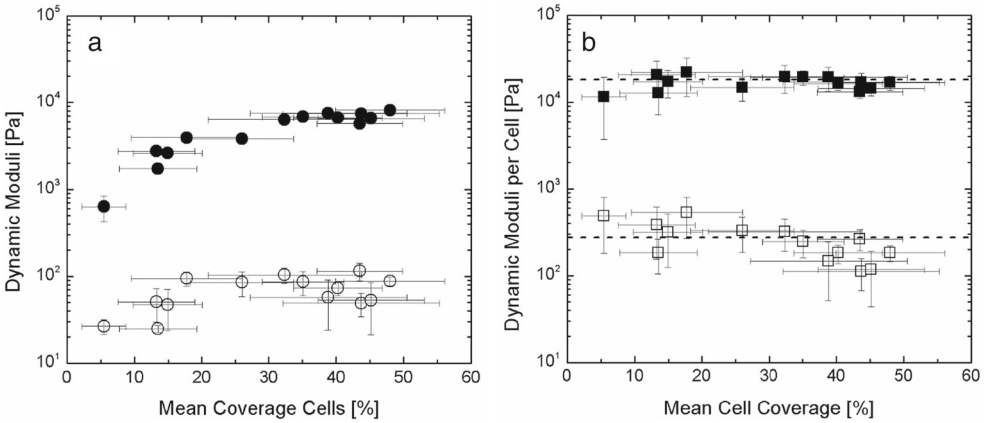

Fig. 4 Storage modulus and loss modulus of the murine fibroblasts in the linear viscoelastic regime obtained from amplitude sweeps (**a**) and average moduli per cell (**b**) as a function of the cell coverage. Storage modulus and loss modulus are indicated by *closed* and *open symbols*, respectively. The *dashed lines* in (**b**) indicate the mean values of the data points for the respective moduli. Gap width, 5 μm; frequency, 1 Hz

Figure 5a shows the normal force, F_N, on the plates as a function of gap width. It is positive at the gap width of 5 μm and negative at larger gaps indicating cell compression at the narrowest gap and elongation at larger gaps. Incremental changes in the normal force are large at small deformations and decrease at larger deformations. With the detected cell coverage, the normal stress per cell, $\langle\sigma_{cell}\rangle$, can be determined analogously to the dynamic moduli.

$$\langle\sigma_{cell}\rangle = -\frac{F_N}{cA} \tag{2}$$

where A is the surface area of the upper plate. Hence, the normal stress per cell ranges from about −1 kPa at a 5-μm gap width to about 7 kPa at a 16-μm gap width.

As shown in Fig. 5b, the pre-set strain has a strong impact on the dynamic moduli. The dynamic moduli strongly decrease with increasing gap width. At a gap width of 16 μm, the storage modulus is about a factor of 50 smaller than at 5 μm. Returning from the maximum gap width to the minimum one at the end of the experiment, the initial high storage modulus is almost recovered: The decrease of about 18 % is supposed to be due to detachment of a corresponding amount of cells during the elongation phase. In this case, the tensile stress at maximum gap width increases to about 8 kPa.

Figure 6a depicts exemplary frequency sweeps for different gap widths. The larger the gap width, the stronger the moduli increase with frequency. Figure 6b shows the exponent of a power-law fit to the data. Both exponents increase with gap width where the exponent of the storage modulus is somewhat larger than that of the loss modulus.

To clarify the impact of the cell nucleus on the rheological study, we treated the cells with blebbistatin. Compared to untreated cells, the storage modulus is lowered by blebbistatin by a factor of 2.5. The loss modulus was hardly altered within range of uncertainty. In the frequency sweeps, blebbistatin treatment yields much smaller exponents of about 0.065 and 0.04 for the power-law behavior of the storage and loss moduli, respectively.

As shown in Fig. 7a, the mean size of human fibroblasts for the different passages increases from about 12 μm to about 18 μm with the number of passages. Therefore, we adopted the gap width and carried out the rheological studies at normal forces close to zero (0.01–0.03 N) to avoid the strong impact of pre-stress shown in Fig. 5b. The storage modulus of the single runs also seems to increase. Yet, as shown in Fig. 7b, it remains within a corridor of a factor of 2, a range found for the murine fibroblasts in Fig. 4b.

Figure 8 comprises the storage moduli per cell of the three different cell types. Since the values for the different passages

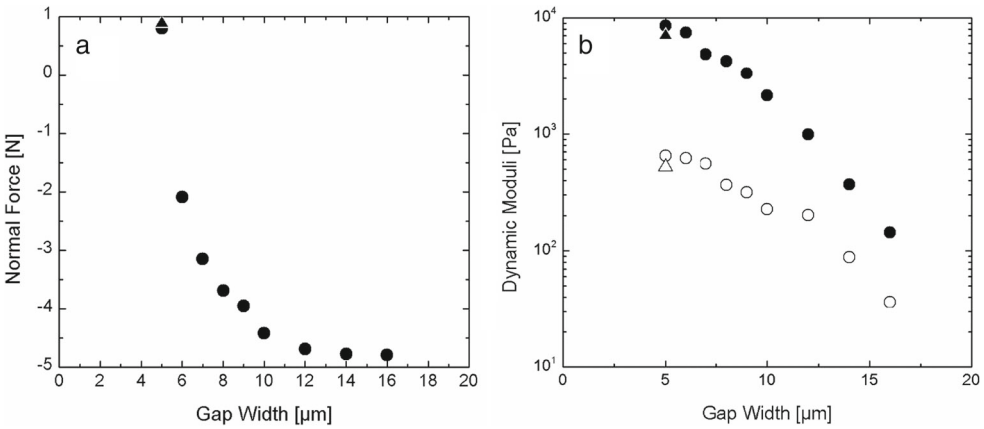

Fig. 5 Gap-width dependency of the normal force (**a**) and of the dynamic moduli (**b**) in the linear viscoelastic range for mouse fibroblasts. The experiment was carried out by stepwise increasing the gap width from 5 μm to larger gap widths. In (**b**), the *closed* and *open symbols* show the storage and loss moduli, respectively. The *triangles* show the data measured at the end of the experiment at a 5-μm gap width. Cell coverage, 36 %; strain amplitude, 0.2 %; frequency, 1 Hz

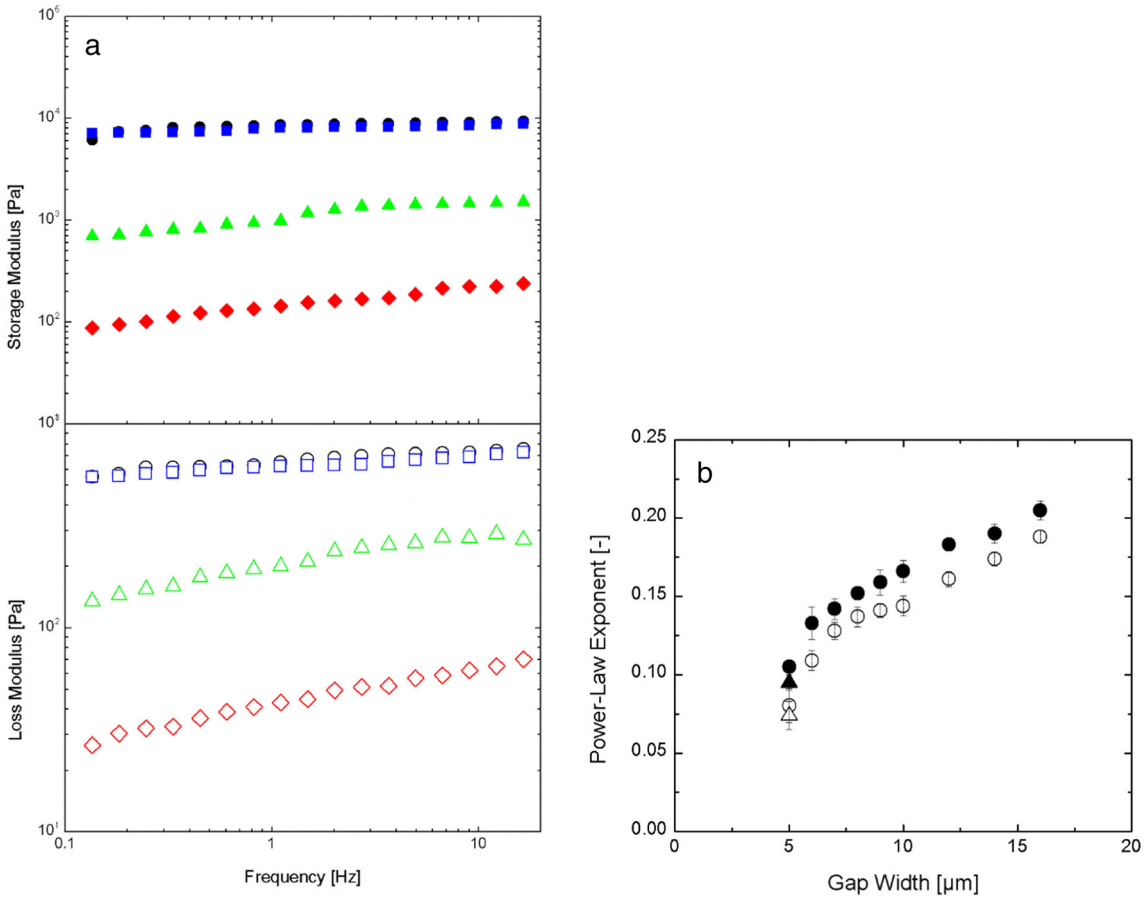

Fig. 6 Frequency sweeps (**a**) and their power-law exponents (**b**) as a function of the gap width for mouse fibroblasts. The experiment was carried out by stepwise increasing the gap width from 5 μm to larger gap widths. *Closed* and *open symbols* show the data for the storage and the loss moduli, respectively. In (**a**), (*black*) *circles* and (*blue*) *squares* indicate the moduli at a gap width of 5 μm at the beginning and at the end of the experimental run, respectively; (*green*) *triangles* and (*red*) *diamonds* indicate the moduli at a gap width of 10 and 16 μm, respectively. The *triangles* in (**b**) show the data measured at the end of the experiment at a 5-μm gap width. Cell coverage, 36 %; strain amplitude, 0.2 %

of the human fibroblasts remain within a corridor of a factor of 2, we did not distinguish between them in this diagram. They group around the mean value with a standard deviation of about 24 %. The human fibroblasts have an average storage modulus that is about a factor of 2.8 lower than that of the mouse. The HeLa cells, on the other hand, have a storage modulus that is an order of magnitude smaller than those of the fibroblasts. They group around the mean value with a standard deviation of about 15 %. The loss moduli of the different cell types show the same tendency like the storage modulus. Yet, scatter is considerably larger and mean values differ only by a factor 3–4 between the lowest (HeLa) and highest ones (mouse fibroblasts).

Discussion

Quite a number of different techniques are used to study the rheological properties of single cells. Yet, due to large cell-to-cell variations, a considerable number of cells have to be studied to obtain statistically robust data on average values and to quantify the impact of drug treatment or of diseases on the rheological cell properties. Instead of numerous sequential experimental runs, it is desirable to obtain this data from a single sweep. In particular, it seems appealing to apply well-established techniques and the versatility of commercial rheometers. In a former study, Fernández et al. (2007) showed the ability to measure rheological properties with a rotational rheometer. They carried out amplitude and frequency sweeps with a monolayer of a large number of fibroblast cells. They studied, however, the nonlinear viscoelastic regime at rather large amplitudes and, since they did not determine the number of cells, quantitative information on cell moduli cannot be extracted from their measurements.

To determine average rheological cell properties, we used the narrow-gap rheometer recently described by Dakhil and Wierschem (2014). It allows setting up gap widths of a few micrometers in the parallel-disk configuration and thus allows studying the rheological behavior of the cells under pre-set stress conditions. To quantify the average cell properties, it

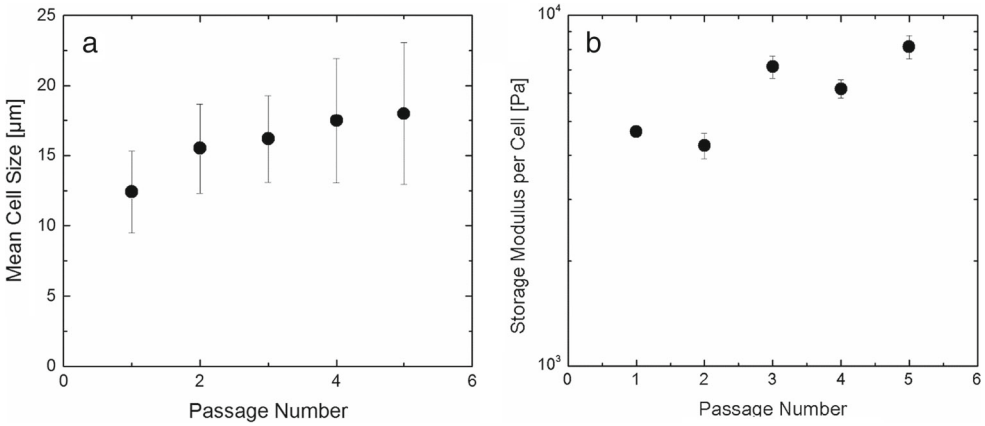

Fig. 7 Mean size (**a**) and storage modulus per cell (**b**) of human fibroblasts for the different passages. *Error bars* in (**a**) indicate standard deviation

is necessary to detect the cell coverage in the monolayer. As shown in Fig. 4, it is indeed possible to obtain average storage and loss moduli for the cells for a large range of the cell coverage between a few percent up to about 50 %. The main restrictions seem to be rheometer's torque resolution at low and multilayers at high cell coverage. A cell coverage of about 30–50 % seems to be optimal. Within the studied range, the moduli per cell are independent of cell coverage. The storage modulus per cell varies by less than a factor of 2 between the single measurements; see Fig. 8. The standard deviation for the cell storage modulus is about 20 %. This is much smaller than typical cell-to-cell variations (Cai et al. 2013). As is apparent from Fig. 4, the main uncertainty originates from variations in the cell distribution; see also Fig. 1b. Hence, it seems near at hand that improving cell distribution may noticeably improve reproducibility further.

The entire measurement time for amplitude and frequency sweeps is about 30 min. As was checked with HeLa cells and propidium iodide, there are hardly any dead cells in the monolayer. The number of dead cells was about 2 % and barely altered during the sweeps. A rheological measurement at fixed frequency and amplitude just takes a few seconds. It was pointed out that the cytoskeleton's mechanical properties may be affected due to aging processes (Schulze et al. 2010). Yet, as shown in Fig. 3, the rheological properties of the cells hardly change during the time interval of the sweeps. The storage modulus increases slightly during the first 200 min and remains rather constant for the rest of the 10 h lasting experimental run while the loss modulus remains rather constant during the entire experiment. We expect that rather large recording times can be realized due to the fact that the cells are still within their medium, of which the contribution to the rheological measurements is negligible. However, long-term effects of the measurement on cell viability were not tested.

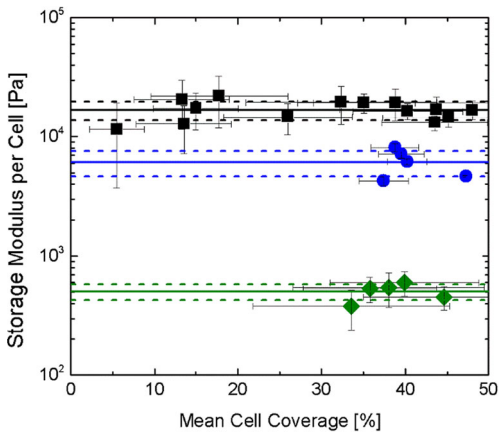

Fig. 8 Storage modulus per cell of mouse fibroblasts (*black squares*), human fibroblasts (*blue circles*), and HeLa cells (*green diamonds*). *Solid lines* show the mean modulus, *thin dashed lines* indicate the range within standard deviation between the measurements

To compare the storage moduli of different cells quantitatively, reaching the linear viscoelastic regime is mandatory. We showed that it is possible to study the linear viscoelastic regime with the monolayer configuration. Figure 2 reveals that the linear viscoelastic regime of our cells extends to amplitudes of less than 1 %. For the fibroblasts, however, Fig. 2a displays strong scattering for the loss modulus at low strain amplitudes making it difficult to obtain precise data for this quantity in the linear viscoelastic regime. Therefore, in amplitude sweeps, the loss modulus in the linear viscoelastic regime was determined from its valley in the strain amplitude range between 0.3 and 1 %. A comparison to the HeLa cells in Fig. 2b, which have much smaller moduli, shows that the scatter is apparently not due to the torque limit of the used rheometer. The absence of the strong scatter also in fibroblasts at larger gap widths may point to the fact that the nucleus may interfere resulting in larger friction.

Although the murine cells are slightly compressed at a gap of 5 μm, the data on the storage modulus at this gap width is apparently due to the cytoskeleton and not due to the nucleus: In treating the cells with blebbistatin, which acts specifically on the cytoskeleton inhibiting myosin-II ATPase but does not directly interfere with the nucleus, we see a considerable weakening of the storage modulus. Furthermore, comparing the normal forces at a gap width of 5 μm with that of 6 μm

(Fig. 5a), shows that the cells are only slightly compressed. If the nuclei were affected, we would expect a much higher absolute value for the normal force since the nucleus is considerably stiffer than the cytoskeleton (Guilak et al. 2000; Caille et al. 2002; Pajerowski et al. 2007). In that case, one would expect a much higher increase of the dynamic moduli for compressed cells compared to elongated ones. Yet, compared to the cytoplasm, a 3–10 times higher stiffness has been reported for the nuclei (Guilak et al. 2000; Caille et al. 2002), while the increase of the storage modulus between gap widths of 7 and 5 μm is less than a factor of two.

The treatment with blebbistatin also shows that the approach is suitable to quantify the impact of drug treatment on cell rheology. It does not resolve single-cell mechanistics by this treatment but compares different cell samples. Inhibiting myosin-II motors with blebbistatin rather lowers the storage modulus compared with untreated cells, which is consistent with findings in single-cell studies (Balland et al. 2005; Kasza et al. 2009; Mitrossilis et al. 2009). Furthermore, we observe that the power-law exponents of the blebbistatin-treated cells are considerably lower than those of the untreated cells. In particular, similar to the behavior of myoblasts treated with blebbistatin found by Balland et al. (2005), the power-law exponent for the loss modulus is smaller than that for the storage modulus.

The storage and loss moduli in the linear viscoelastic regime as well as their power-law exponent strongly depend on the gap width and thus on the pre-set stress created by elongating or compressing the cells with the rheometer plates (Figs. 5 and 6). Increasing the gap width for mouse fibroblasts from 5 to 16 μm results in a decrease of the moduli by more than an order of magnitude. Comparison between initial and final measurement of the storage modulus at minimum gap width indicates a detachment of about 18 % of the cells during the entire elongation process, which has only a minor effect compared to the drastic decline of the dynamic moduli at larger gaps.

It is apparent from Fig. 5a that the cells are slightly compressed at a gap width of 5 μm and elongated at larger gap widths. Taking a gap width with zero normal force as reference, the maximum gap width studied corresponds to a stretch ratio of about 3. With the detected cell concentration, normal stresses ranging from −1 kPa to about 7–8 kPa are obtained. In the studied range, the normal force and hence the normal stress show a nonlinear dependence on the gap width. The weaker increase of the absolute normal force at larger elongations cannot be explained by cell detachment as quantified from the data for the storage modulus and rather indicates softening of the cells at larger elongation. This behavior was also reported for single cells during a stepwise increase of elongation (Micoulet et al. 2005). These authors also found for 3T3 fibroblasts at a temperature of 310 K normal stresses in the range of a few kilopascals.

Many rheological studies focus on frequency-dependent cell properties. In a wide frequency range, they usually find a power law for rheological quantities, such as the storage or loss modulus that is typical for soft glassy materials. The exponents are smaller for stiffer cells (see Kollmannsberger and Fabry (2011) and references therein). Our frequency sweeps are in accordance with these findings (Fig. 6). The values are in the range typically found for the linear viscoelastic regime of animal cells. Yet, we find that the exponent for the loss modulus tends to be somewhat smaller than that for the storage modulus (Fig. 6b). We hypothesize that this might be due to considerable scatter for the loss modulus at the small strain amplitudes studied.

The human fibroblasts increase in mean size during the first passages (Fig. 7a). Increasing mean cell size with passages has been correlated to a loss of proliferation (Mitsui and Schneider 1976; Greenberg et al. 1977). As shown in Fig. 7b, this is accompanied by an increase in the average storage modulus, in line with the observation of a considerable increase in stiffness of epithelial cells at high passage numbers (Berdyyeva et al. 2005). Figure 8 shows that the studied cells differ considerably in their storage moduli. The observation that the human fibroblasts have a storage modulus that is more than a factor of 2 lower than the murine fibroblasts may be attributed to species-specific differences. Concerning the cancer cell line, the storage modulus of the HeLa cells is an order of magnitude smaller than that of the fibroblasts. This is in line with earlier observations of dramatically softer cancer cells (Lekka et al. 1999; Guck et al. 2005) and reflects the ability of strong proliferation of cancerous cells. The lower mechanical strength of exuberantly growing cancer cells can be traced back to reduced actin polymerization (Guck et al. 2005).

Conclusions

We showed that in modifying a commercial rheometer to set up a parallel-disk configuration at gap widths of a few micrometers and detecting optically the cell concentration within the gap, it is possible to determine typical average dynamic cell moduli in the linear viscoelastic range with a rotational rheometer. The average cell properties can be detected in a large range of cell concentrations. A coverage of 30–50 % is most advantageous. Changing the gap width and measuring the normal force with the rheometer, the cells may be compressed or elongated and the impact of pre-stress on the cell properties can be quantified. This may path the way to use the method as a diagnostic tool to study quantitatively average rheological cell properties and how they are affected by biochemical treatment or by diseases, e.g., in cancer cells. With this method, we quantified differences in the rheological properties between murine and primary human fibroblasts and cancerous HeLa cells.

Acknowledgments H. D. gratefully acknowledges the financial support by Deutscher Akademischer Austauschdienst (DAAD), Germany, and the Ministry of Higher Education and Scientific Research, Iraq. H. E. gratefully acknowledges the financial support by the Federal Ministry of Education and Research (BMBF), Germany, under project number 031A305E. We thank Mr. J. Heubeck and Mr. H. Weber for implementing the setup and S. Schürmann for the helpful discussions.

References

Balland M, Richert A, Gallet F (2005) The dissipative contribution of myosin II in the cytoskeleton dynamics of myoblasts. Eur Biophys J 34:255–261

Berdyyeva TK, Woodworth CD, Sokolov I (2005) Human epithelial cells increase their rigidity with ageing in vitro: direct measurements. Phys Med Biol 50:81–92

Cai P, Mizutani Y, Tsuchiya M, Maloney JM, Fabry B, van Vliet KJ, Okajima T (2013) Quantifying cell-to-cell variation in power-low rheology. Biophys J 105:1093–1102

Caille N, Thoumine O, Tardy Y, Meister J-J (2002) Contribution of the nucleus to the mechanical properties of endothelial cells. J Biomech 35:177–187

Dakhil H, Wierschem A (2014) Measuring low viscosities and high shear rates with a rotational rheometer in a thin-gap parallel-disk configuration. Appl Rheo 24:63795

Davies GA, Stokes JR (2005) On the gap error in parallel plate rheometry that arises from the presence of air when zeroing the gap. J Rheol 49: 919–922

Davies GA, Stokes JR (2008) Thin film and high shear rheology of multiphase complex fluids. J. Non-Newtonian Fluid Mech 148:73–87

Elkins CM, Shen W-J, Khor VK, Kraemer FB, Fuller GG (2015) Quantification of stromal vascular cell mechanics with a linear cell monolayer rheometer. J Rheol 59:33–50

Fernández P, Heymann L, Ott A, Aksel N, Pullarkat PA (2007) Shear rheology of a cell monolayer. New J Phys 9:419

Freshney RI (1993) Culture of animal cells. A manual of basic techniques. 3rd ed. Wiley-Liss, New York

Gey GO, Coffmann WD, Kubieck MT (1952) Tissue culture studies of the proliferative capacity for cervical carcinoma and normal epithelium. Cancer Res 12:264–265

Gilbert DF, Meinhof T, Pepperkok R, Runz H (2009) DetecTiff: a novel image analysis routine for high-content screening microscopy. J Biomol Screen 14:944–955

Greenberg SB, Grove GL, Cristofalo VJ (1977) Cell size in aging monolayer cultures. In Vitro 13:297–300

Grinell F (1994) Fibroblasts, myofibroblasts, and wound contraction. J Cell Biol 124:401–404

Guck J, Schinkinger S, Lincoln B, Wottawah F, Ebert S, Romeyke M, Lenz D, Erickson HM, Ananthakrishnan R, Mitchell D, Käs J, Ulvick S, Bilby C (2005) Optical deformability as an inherent cell marker for testing malignant transformation and metastatic competence. Biophys J 88:3689–3698

Guilak F, Tedrow JR, Burgkart R (2000) Viscoplastic properties of the cell nucleus. Biochem Biophys Res Comm 269:781–786

Karimi A, Navidbakhsh M, Haghighatnama M, Motevalli Haghi A (2015) Determination of the axial and circumferential mechanical properties of the skin tissue using experimental testing and constitutive modeling. Comp Meth Biomech Biomed Engg 18:1768–1774

Kasza KE, Nakamura F, Hu S, Kollmannsberger P, Bonakdar N, Fabry B, Stossel TP, Wang N, Weitz DA (2009) Filamin A is essential for active cell stiffening but not passive stiffening under external force. Biophys J 96:4326–4335

Kollmannsberger P, Fabry B (2009) Active soft glassy rheology of adherent cells. Soft Matter 5:1771–1774

Kollmannsberger P, Fabry B (2011) Linear and nonlinear rheology of living cells. Annu Rev Mater Res 41:75–97

Kovács M, Tóth J, Hetényi C, Málnási-Csizmadia A, Sellers JR (2004) Mechanism of blebbistatin inhibition of myosin II. J Biol Chem 279: 35557–35563

Lekka M, Laidler P, Gil D, Lekki J, Stachura Z, Hrynkiewicz AZ (1999) Elasticity of normal and cancerous human bladder cells studied by scanning force microscopy. Eur Biophys J 28:312–316

Lucey BP, Nelson-Rees WA, Hutchins GM (2009) Henrietta lacks, HeLa cells, and cell culture contamination. Arch Path Lab Med 133:1463–1467

Masters JR (2002) HeLa cells 50 years on: the good, the bad and the ugly. Nat Rev Cancer 2:315–319

Micoulet A, Spatz JA, Ott A (2005) Mechanical response analysis and power generation by single-cell stretching. Chem Phys Chem 6: 663–670

Mierke CT, Kollmannsberger P, Paranhos Zitterbart D, Smith J, Fabry B, Goldmann WH (2008) Mechano-coupling and regulation of contractility by the vinculin tail domain. Biophys J 94:661–670

Mitrossilis D, Fouchard J, Guiroy A, Desprat N, Rodriguez A, Fabry B, Asnacios A (2009) Single-cell response to stiffness exhibits muscle-like behavior. PNAS 106:18243–18248

Mitsui Y, Schneider EL (1976) Relationship between cell replication and volume in senescent human diploid fibroblasts. Mech Ageing Dev 5:45–56

Niu T, Cao G (2014) Power-law rheology characterization of biological cell properties under AFM indentation measurement. RSC Adv 4:29291

Oliveira MS, Yeh R, McKinley GH (2006) Iterated stretching, extensional rheology and formation of beads-on-a-string in polymer solutions. J Non-Newtonian Fluid Mech 137:137–148

Pajerowski JD, Dahl KN, Zhong FL, Sammak PJ, Discher DE (2007) Physical plasticity of the nucleus in stem cell differentiation. PNAS 104:15619–15624

Pan C, Kumar C, Bohl S, Klingmueller U, Mann M (2009) Comparative proteomic phenotyping of cell lines and primary cells to assess preservation of cell type-specific functions. Mol Cell Proteomics 8:443–450

Pipe CJ, Majmudar TS, McKinley GH (2008) High shear rate viscometry. Rheol Acta 47:621–642

Sasaki DT, Dumas SE, Engleman EG (1987) Discrimination of viable and non-viable cells using propidium iodide in two color immunofluorescence. Cytometry 8:413–420

Schulze C, Wetzel F, Kueper T, Malsen A, Muhr G, Jaspers S, Blatt T, Wittern KP, Wenck H, Käs JA (2010) Stiffening of human skin fibroblasts with age. Biophys J 99:2434–2442

Soulages J, Oliveira MS, Sousa PC, Alves MA, McKinley GH (2009) Investigating the stability of viscoelastic stagnation flows in T-shaped microchannels. J Non-Newtonian Fluid Mech 163:9–24

Stamenović D, Rosenblatt N, Montoya-Zavala M, Matthews BD, Hu S, Suki B, Wang N, Ingber DE (2007) Rheological behavior of living cells is timescale-dependent. Bio J 93:L39–L41

Todaro GJ, Green H (1963) Quantitative studies of the growth of mouse embryo cells in culture and their development into established lines. J Cell Biol 17:299–313

Tuan T-L, Song A, Chang S, Youmai S, Nimni ME (1996) In vitro fibroplasia: matrix contraction, cell growth, and collagen production of fibroblasts cultured in fibrin gels. Exp Cell Res 223:127–134

Unger RE, Krump-Konvalinkova V, Peters K, Kirkpatrick CJ (2002) *In vitro* expression of the endothelial phenotype: comparative study of primary isolated cells and cell lines, including the novel cell line HPMEC-ST1.6R. Microvascular Res 64:384–397

Verdier C, Etienne J, Duperray A, Preziosi L (2009) Review. Rheological properties of biological materials. Comp Rend Phys 10:790–811

Weissman-Shomer P, Fry M (1975) Chick embryo fibroblasts senescence in vitro: pattern of cell division and life span as a function of cell density. Mech Ageing Dev 4:159–166